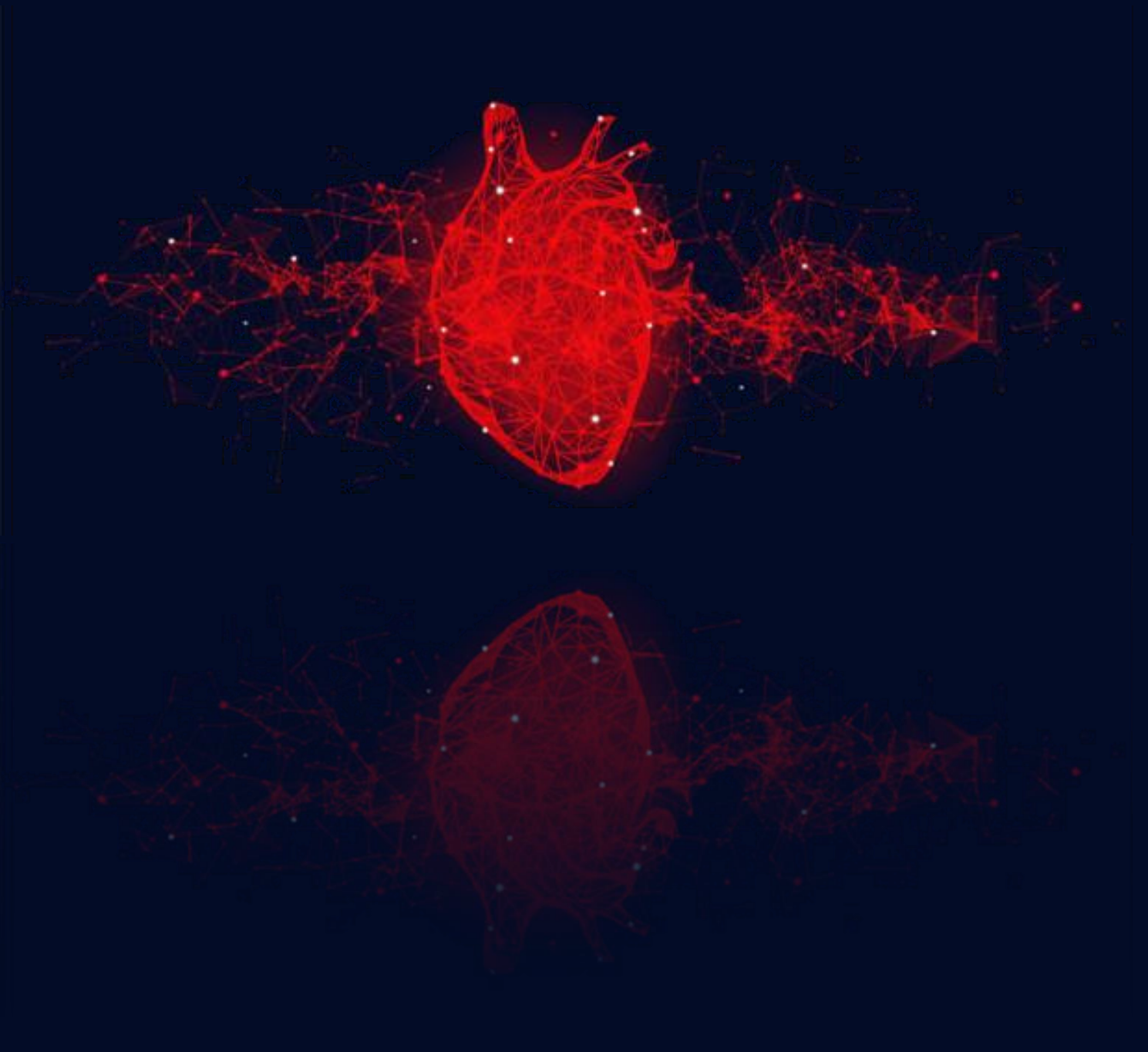


Chapter 2

Investigating miR34a-5p – Clock synergy and its proatherogenic implications



Introduction

The circadian system in organisms temporally orchestrates rhythmic changes in a vast number of genes and gene products in different organs. Multifaceted interactions amongst these components, both at inter- and intra-cellular levels, ultimately lead to rhythmic behaviour and physiology. Identifying the plethora of circadian targets and mapping their interactions with one another is essential to comprehend the molecular mechanisms of circadian regulation and its pathological implications. The positive arm of circadian feed-back loop systems comprises of CLOCK and BMAL1, wherein they form a heterodimer on SIRT1 assisted deacetylation of BMAL1 to bind to the E-box and initiate transcription of Clock Controlled Genes (CCGs). The CCGs forming a part of core clock system encompass Period family (PER1, PER2, PER3) and Cryptochrome family (CRY1, CRY2). This feedback loop system is further fine-tuned by participation of key controlling factors miRNAs. miRNAs have not only been reported for their potential regulation of gene expression but also has been shown to have a regulatory role on length of the circadian clock period. miR192/194 cluster is reported to regulate period gene family and circadian rhythms (Nagel *et al.*, 2009). miR397 has been documented to maintain circadian feedback loop systems in normal physiology (Feng *et al.*, 2020). miR132 mediated chromatin remodelling and manifestation of translational control of circadian clock has also been reported (Alvarez-Saavedra *et al.*, 2011). miR34a-5p has been reported to regulate both PER1 and PER2 gene expression and potentially regulate circadian rhythm (Han *et al.*, 2016). Overexpression of miR34a-5p inhibiting PER2 is also stated responsible for altering circadian period length (Hasakova *et al.*, 2019).

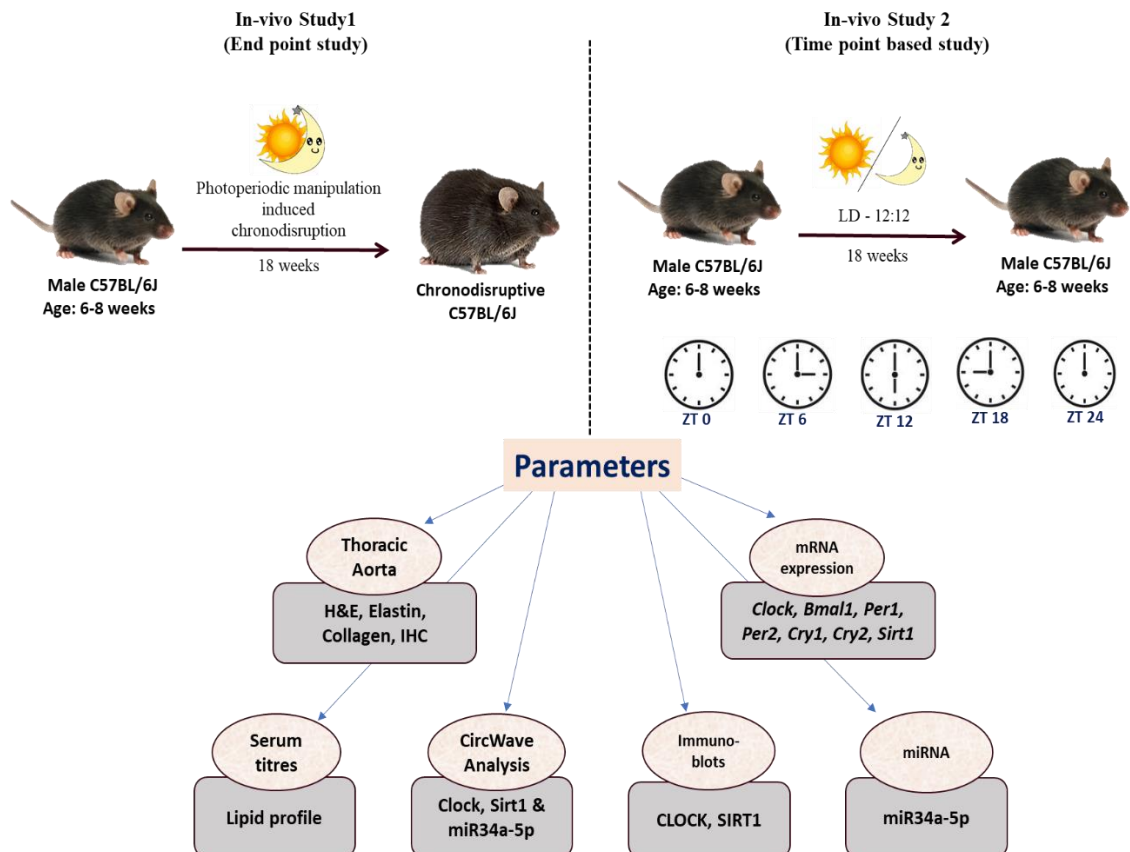
Along with a chief contribution in methodically regulating operation of circadian rhythms CLOCK is also implicated in manifesting cognitive functions and regulating metabolism. CLOCK dimerise with BMAL1 and manifest translation of key metabolic regulatory genes viz. Rev-erb α ; regulating bile acid and lipid metabolism, PPAR α ; regulating fatty acid metabolism, Shp; regulating lipid and bile acid metabolism, USF2 regulating cholesterol efflux in macrophages, Gata4 regulating cholesterol efflux into bile etc. Dominant CLOCK mutant mice exhibited macrophages with higher tendency of taking up oxidized lipid and impaired cholesterol efflux capabilities via Usf2 (Pan *et al.*, 2020). Mutant CLOCK also disrupts the circadian entrainment and food entrainment of clock genes. Furthermore, disrupted CCG production subsequently manifest in detrimental effects including elevated LDL in circulation, disturbed VLDL secretion and circulation, elevated cholesterol, and metabolic shift to obesity. A study shows that a total of 100 of 663 metabolites, representing all metabolite categories, showed diurnal rhythmic concentrations that exceeded the Bonferroni threshold, showing that the peak times of all phospholipids were clustered during the afternoon to midnight (Gu *et al.*, 2019).

Persistently altered metabolism eventually culminates into some or the other kind of cardiovascular disfunction. This compile of study focuses on investigated circadian impact on atherosclerosis with the lens of miRNA modulators. Circadian fluctuations of glucocorticoids, catecholamines, blood viscosity, and platelet reactivity have been well established in humans and correlate with plaque rupture and thrombus formation in the early morning hours (Steffens *et al.*, 2017). Multiple triggering factors viz. expression of adhesion molecules, chemokines, leukocytes, and hormones have also been associated to progression of atherosclerosis.

In previous chapter we had identified miR34a-5p as a potential miRNA regulating CLOCK gene with pro-atherogenic tendencies using computational algorithms and databases. Herein, we aim to validate miR34a-5p – CLOCK interaction and its impact on pro-atherogenic manifestations using in-vivo (thoracic aorta of C57BL/6J mice) and in-vitro (HUVEC cells representing intimal layer of the aortae) experimental model systems. Furthermore, an attempt to evaluate circadian rhythm of physiological expression of miR34a-5p in murine and cellular systems has also been studied by doing time point based expressional evaluations of miRNA and its target mRNAs.

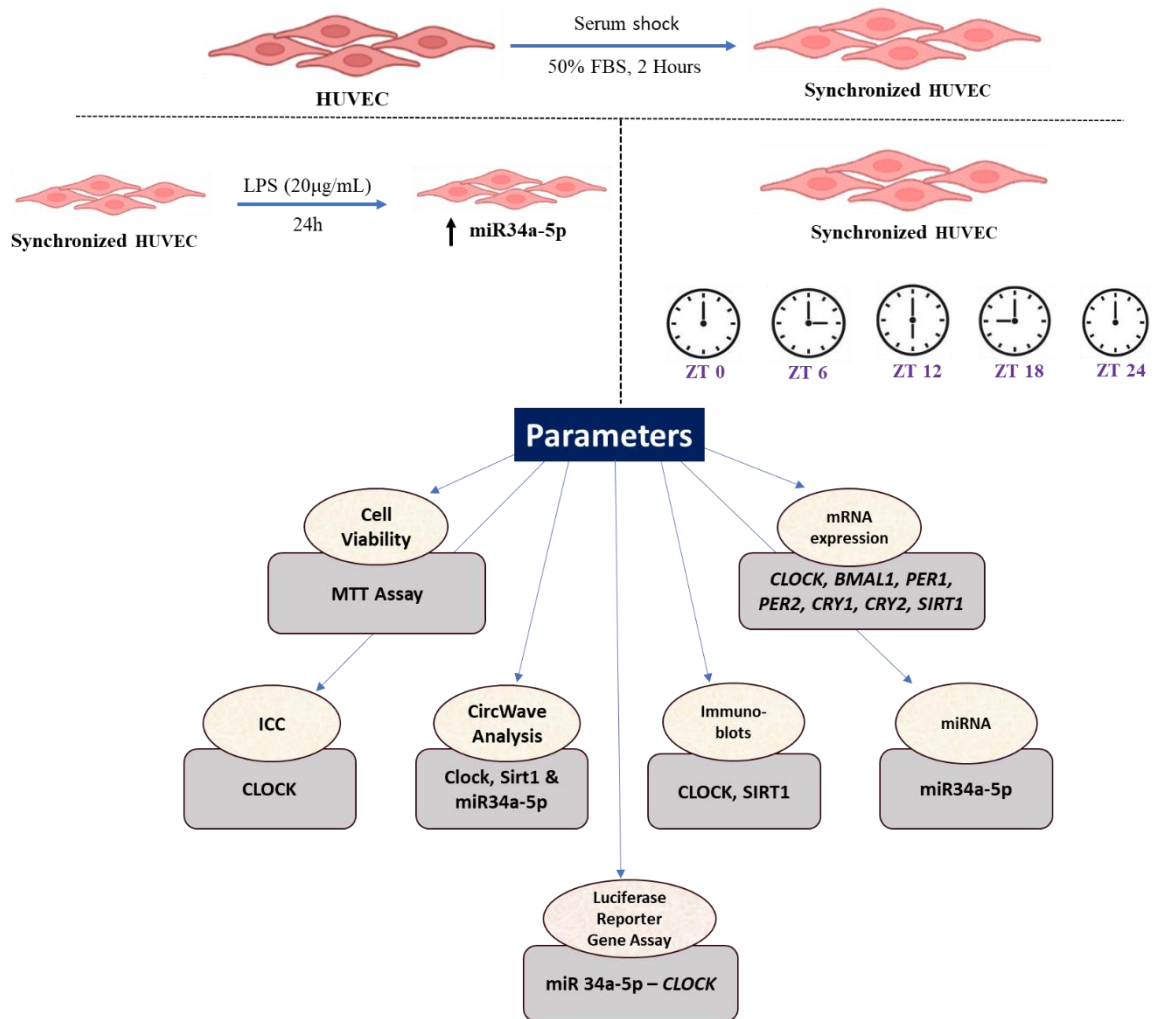
Methodology

In-vivo Experimentations



The detailed protocol and pictorial representation of phase advance/ phase delay photoperiodic regimen used for induction of chronodisruption in male C57BL/6J mice has been illustrated in section – Material and Methods.

In-vitro Experimentations



Results

Photoperiodic manipulation induced chronodisruption in C57BL/6J mice

C57BL/6J mice were subjected to phase advance/phase delay photoperiodic regimen for a period of 18 weeks (Joshi *et al.*, 2021). At the end of the experiment thoracic aorta was collected at ZT 0 and assessed for circadian clock genes. Transcriptomal analysis of *Clock*, *Bmal1*, *Per1*, *Per2*, *Cry1* and *Sirt1* showed lowered expression in CD group as compared to control. Whereas *Cry2* levels were elevated (Fig 2.1a). Immunoblot analysis of CLOCK, BMAL1 and SIRT1 exhibited similar expression patterns as seen at transcript level (Fig 2.1b). CLOCK expression as assessed with immunohistochemistry of thoracic aorta showed lowered expression in CD mice as compared to control, further validating the results of mRNA and protein expression (Fig 2.1c).

Chronodisruption induced hypomethylation and consequential elevation of miR34a-5p in thoracic aorta of CD mice.

Thoracic aortae of C57BL/6J mice subjected to CD were assessed for miR34a-5p levels. Titers of miR34a-5p were found to be elevated in the CD mice as compared to that of the control (Fig 2.2a). Chronodisruption is known to cause epigenetic alterations in biological systems. Exploring the plausibility, MSP assay was performed to assess any epigenetic modification in the promoter region of miR34a using different set of primers for methylation and unmethylation with an internal control at CpG island. A significantly lowered methylation was observed in the thoracic aortae of CD mice, coupled with elevated unmethylated region in the same (Fig 2.2b). Cumulatively,

hypomethylation in the promoter region of miR34a plays a role in transcriptional elevation in thoracic aorta of CD mice.

Circadian expression of miR34a-5p and its target genes *Clock* and *Sirt1*

Circadian correlation of miR34a was assessed along with its target genes *Clock* and *Sirt1* in the thoracic aorta of C57BL/6J mice with a time point based study. Thoracic aorta of C57BL/6J mice, maintained under LD 12:12, laboratory chow diet and water ad libitum, were collected at different time points (ZT 0, 6, 12, 18, 24). Transcript level evaluation for *Clock* and *Sirt1* showed two synchronous peaks at ZT 0 and ZT 18. Whereas miR34a-5p showed no significant oscillations in 24h period (Fig 2.3a). Immunoblot analysis was in agreement with the mRNA data (Fig 2.3b). Further, CircWave V1.4 based evaluation showed *Sirt1* and *Clock* exhibiting higher amplitudes than miR34a-5p (Fig 2.3c) and similar peak timings (Fig 2.3d).

Chronodisruption predisposed pro-atherogenic alterations in thoracic aortae of CD mice

Chronodisruption is an established causative factor for atherosclerosis. Further, elevated miR34a-5p and lowered SIRT1 titers have also been reported to promote pro-atherogenic manifestations in different model systems. So herein we decided to evaluate pro-atherogenic manifestations in the thoracic aorta of C57BL/6J mice harboring elevated miR34a-5p and lowered SIRT1 titers. Mild visceral adipose tissue deposits were observed in CD mice (Fig 2.4a). However, it showed non-significant changes in body weight, body circumference (Fig 2.4b & c) and food and water intake

(Fig 2.5a & b). Serum lipid profiles of CD mice showed significant increment in circulating TGs, TCs and LDL and decreased levels of HDL resulting in significantly higher Atherogenic Index of Plasma (AIP) and Cardiac Risk Ratio (CRR) (Fig 2.6a & b).

Gross morphological evaluation of H&E-stained thoracic aortas of CD mice showed intimal derangement and higher intima-media thickening without any atheromatous plaque formation (Fig 2.7a & b). Photomicrographs of elastin autofluorescence showed elastin fragmentation and fibrillar derangement. Further, CD mice recorded significantly higher collagen content (picosirius red stain) and a higher collagen/elastin ratio. The altered collagen-elastin content in CD mice suggest pro-atherogenic changes (Fig 2.8a-c). Overall, the observed microscopic changes in thoracic aorta of CD mice imply towards early proatherogenic changes manifested by the photoperiodic manipulation induced chronodisruption.

mRNA levels of pro-inflammatory genes viz. intercellular adhesion molecule 1 (*Icam1*) and vascular endothelial cell adhesion molecule-1 (*Vcam1*) along with monocyte chemo-attractant protein-1 (*MCP-1*) were significantly upregulated in aorta of CD mice. Whereas mRNA levels of endothelial nitric oxide synthase (*eNOS*) were significantly lower in aortae of CD mice than control. Overall, the data provides further evidence on CD-induced proatherogenic manifestations in thoracic aorta of C57BL/6J mice (Fig 2.9a-d).

Circadian rhythm of miR34a-5p and its target genes in serum synchronized HUVEC

To gauge the circadian rhythm of miR34a-5p and its targets *CLOCK* and *SIRT1* circadian clock of HUVEC cells was synchronized. Cells in invitro cultures do not exhibit circadian behavior in entrained fashion. Herein, HUVECs were subjected to serum shock by treating them with 50% FBS for 2h before experimentations. Serum synchronized HUVECs were harvested at different time points ZT 0, 6, 12, 18 & 24. Where ZT0 was considered at termination of serum shock. miR34a-5p, on assessment exhibited circadian rhythm with two peaks in 24h. The target genes *CLOCK* and *SIRT1* also exhibited circadian expression, which when compares to miR34a-5p showed antagonist synchrony. A single peak was detected at ZT6 and ZT18 for both *CLOCK* and *SIRT1* mRNAs, whereas miR34a-5p showed a circadian pattern with a prominent ebb at ZT6 and ZT18 and peaks at ZT12 and ZT24 (Fig 2.10a & b). This probably exhibits miRNA base inhibition of target gene expression in normal physiological conditions. Further, CircWave software was used to analyze the amplitudes and peak timings, revealing higher amplitude of miR34a-5p as compared to the target genes (Fig 2.10c & d).

LPS induced upregulation of miR34a-5p and consequential decrement in its target genes

LPS is reported to elevate miR34a-5p expression in HUVECs (Zhang *et al.*, 2020). LPS treatment has also been associated to atherogenic studies especially pertaining to inflammation. Considering that LPS was used herein to elevate miR34a-5p levels in HUVEC. Primarily cytotoxic effect of LPS was studied with MTT assay at different

concentrations (2.5, 5, 7, 10, 15 & 20 $\mu\text{g}/\text{mL}$) for deciding the treatment dose. More than 80% cells were viable at concentration of 20 $\mu\text{g}/\text{mL}$ and thus the same was used for further evaluation (Fig 2.11a).

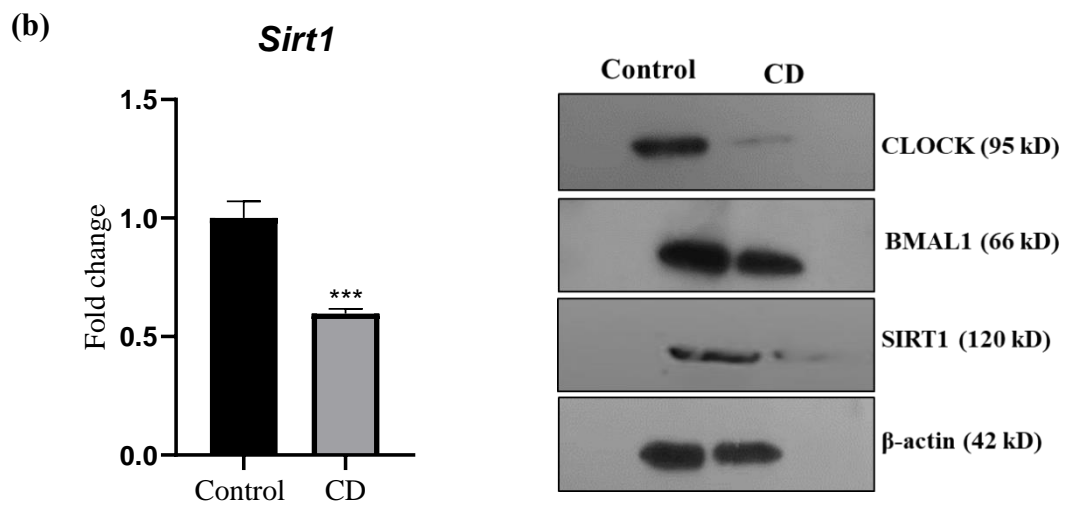
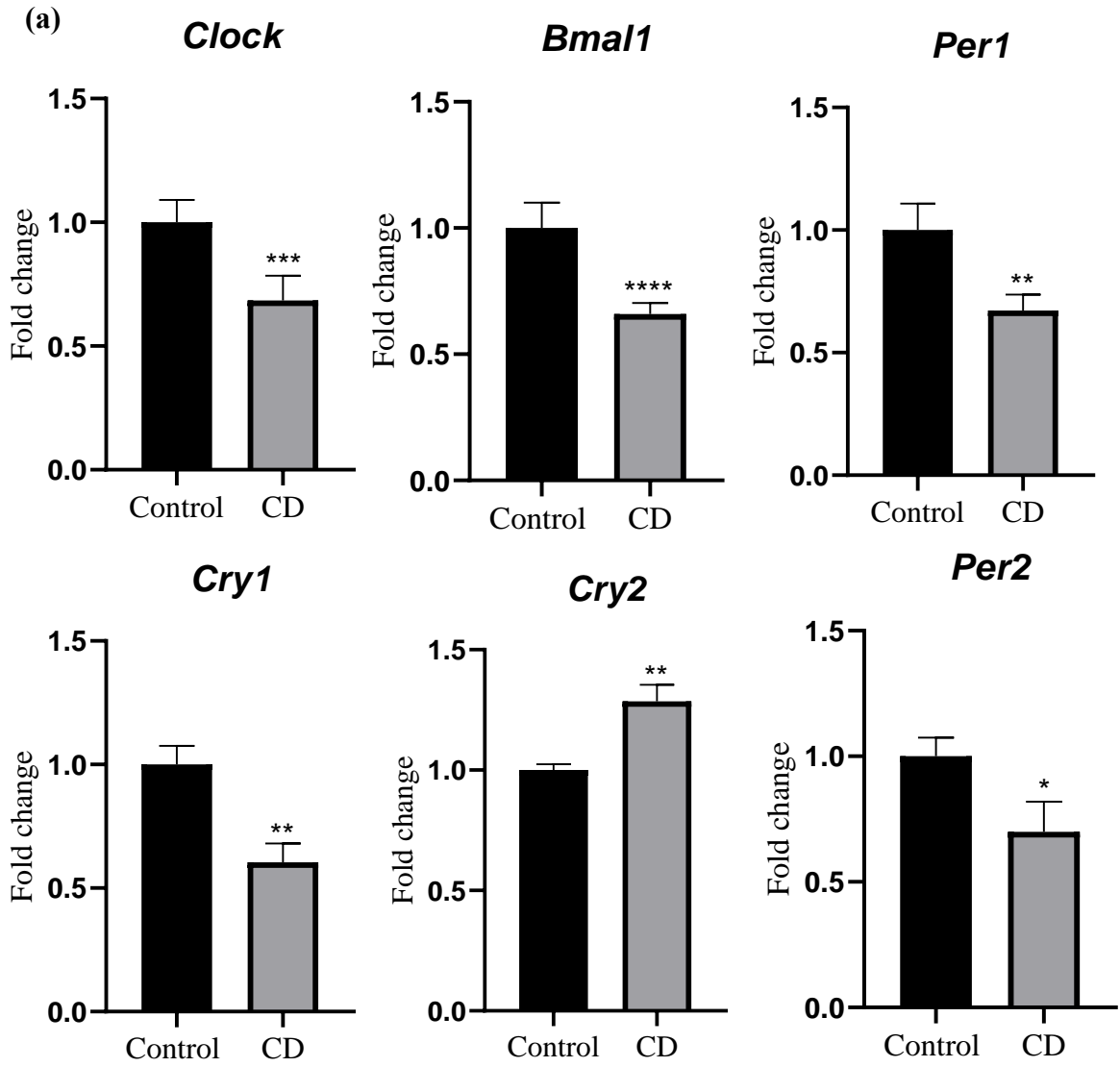
Serum synchronized HUVECs were further treated with 20 $\mu\text{g}/\text{mL}$ of LPS for 24h. Significant increment in miR34a-5p expression was observed in LPS treated cells. The mRNA levels of *CLOCK* and *SIRT1* were comparable to control (Fig 2.11b). However, the protein expression of *CLOCK* and *SIRT1* were found to be significantly lowered (Fig 2.11c). LPS treatment had no impact on transcription of *CLOCK* and *SIRT1* mRNAs. In spite of available transcripts, the same was not translated to protein in the cells harboring higher miR34a-5p that circuitously vouch for miR34a-5p binding to 3'UTR of *CLOCK* and *SIRT1* to inhibit their translation.

Immunocytochemical evaluation of Clock gene in HUVECs harboring elevated miR34a-5p

Serum synchronized HUVECs were treated with 20 $\mu\text{g}/\text{mL}$ of LPS for 24h. These cells were further used for immunocytochemical analysis of *CLOCK* gene. Cells were co-stained with β -actin that served as an internal control and Hoechst 33342 that stained nucleus. LPS treated HUVECs with elevated miR34a-5p showed lowered *CLOCK* expression as compared to that of control adding on as evidence for miR34a-5p – *CLOCK* interactions (Fig 2.12).

miR34a-5p bind to 3'UTR of Clock and alters its expression

In silico data of miR-34a-5p binding to 3'UTR of *CLOCK* gene (Fig 2.13a) and inhibiting its translation was validated in in-vitro system with luciferase reporter gene assay performed on primary endothelial cells. HUVEC cells were co-transfected with miR-34a-5p mimic and plasmid containing a miTarget™ 3' UTR *CLOCK* luciferase reporter. The luciferase activity of the group co-transfected with miR-34a-5p mimic was significantly reduced as compared to those of HUVEC transfected with a scramble miR or with a reporter clone, used as control for off-target effects. Further validation was obtained by co-transfecting miR34a-5p mimic with a mutant reporter clone. Alteration in the seed sequence brought by point mutation (mutant reporter clone) failed to provide Watson-Crick complementarity to miR-34a-5p, allowing full expression of reporter gene and luciferase activity comparable to the scramble control (Fig 2.13b &c). These experiments suggest that miR-34a-5p inhibits *CLOCK* expression by binding to its 3'UTR and inhibiting the translational process.



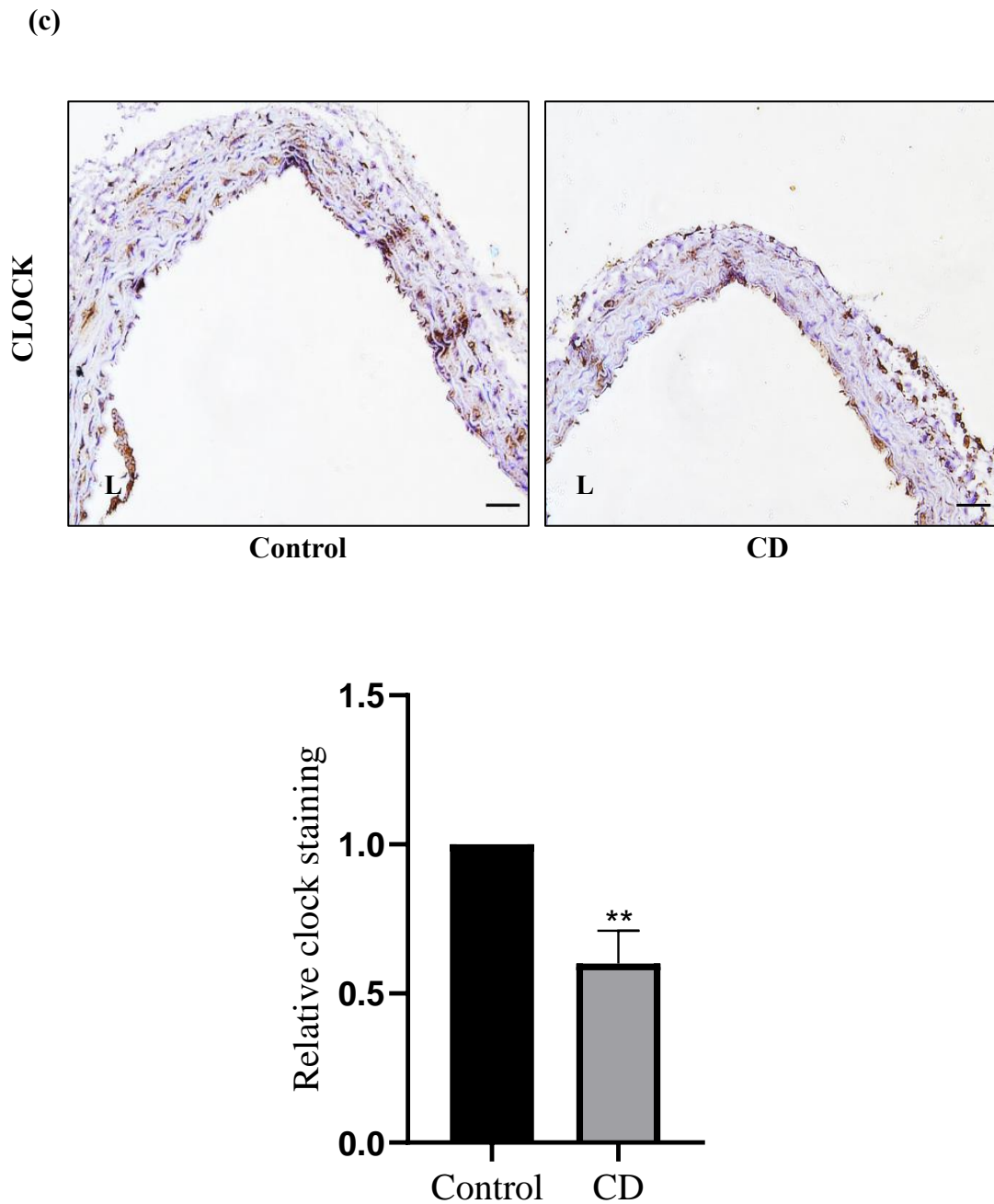


Fig. 2.1: Altered clock gene expression in thoracic aorta of C57BL/6J mice. (a) expression of circadian clock genes quantified at transcript levels (n=5) (b) Immunoblot analysis of key clock genes (n=4) (c) Immunohistochemical analysis of CLOCK gene in the thoracic aorta of mice; L represents luminal area, and the scale is 100 μ m (n=2). Results are expressed as mean \pm S.E.M. * $p < 0.05$, ** $p < 0.01$, *** $p < 0.001$ or **** $p < 0.0001$ is when CD is compared to control group.

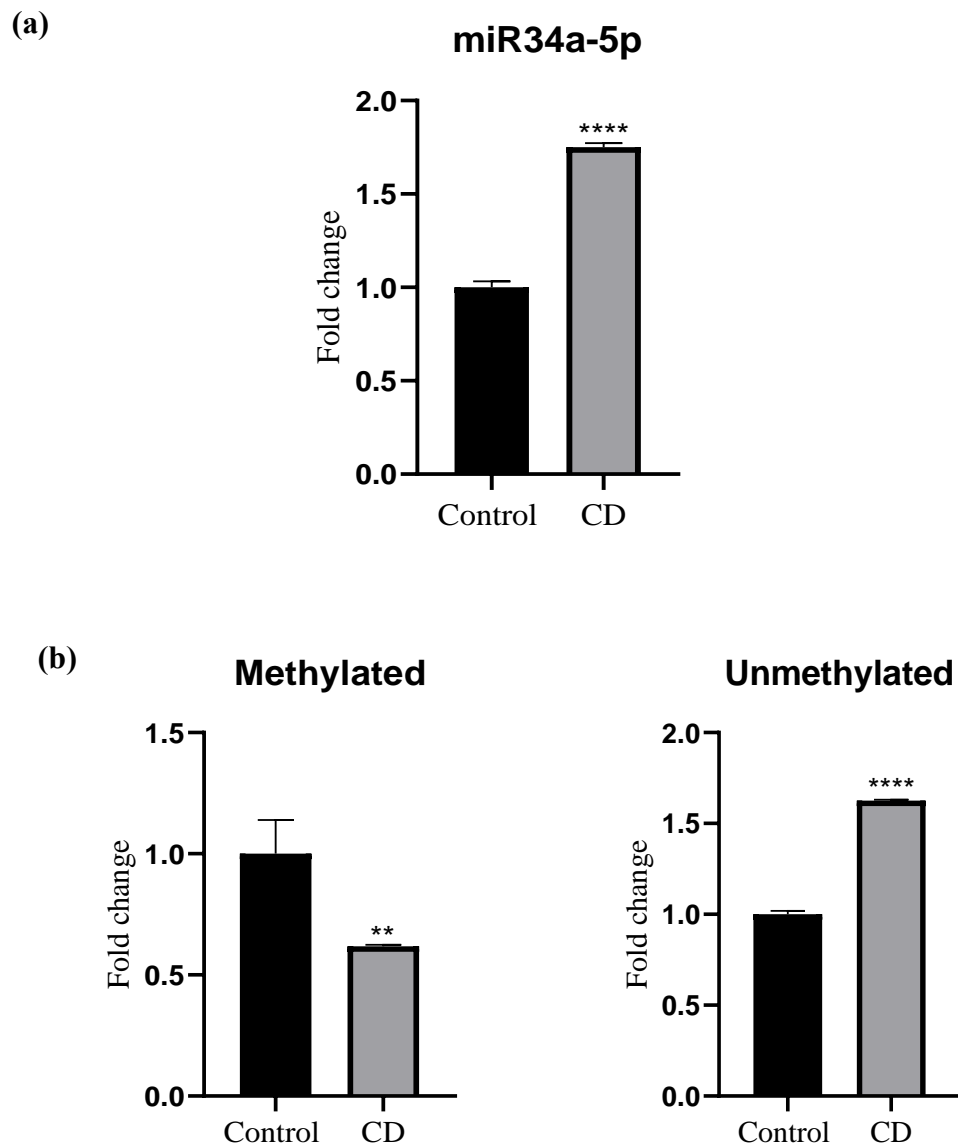
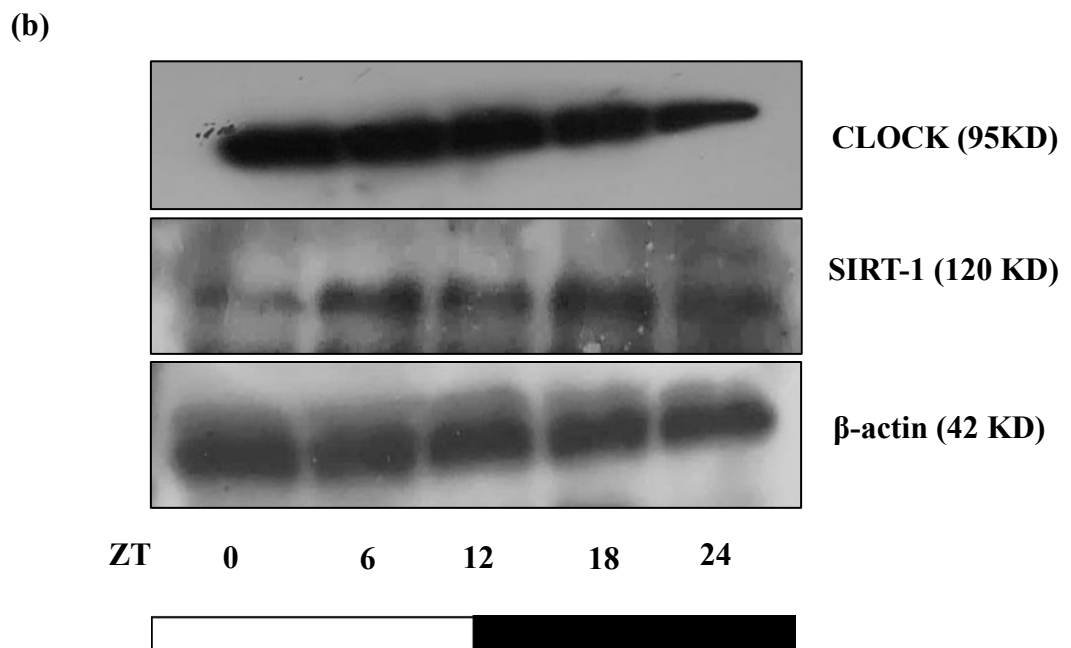
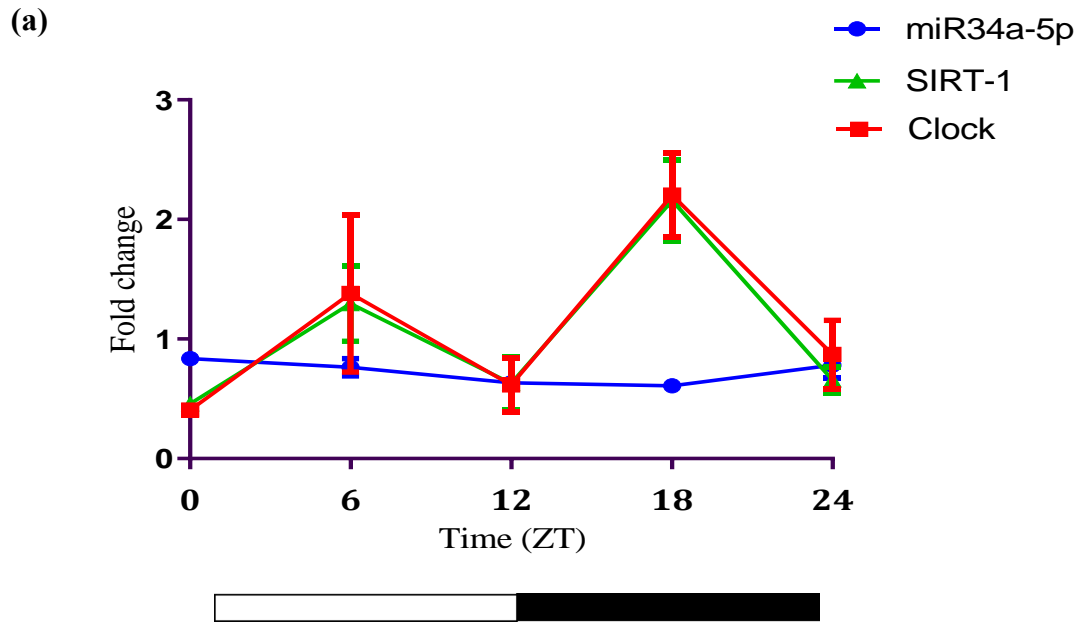


Fig. 2.2: Expression and epigenetic modification at promoter region of miR34a-5p

Thoracic aorta of control and CD mice was assessed for (a) miR34a-5p expression and (b) Modification in the methylation pattern in promoter region of miR34a-5p, evaluated with MSP assay (n=6). Results are expressed as mean \pm S.E.M. * $p < 0.05$, ** $p < 0.01$, *** $p < 0.001$ or **** $p < 0.0001$ is when CD is compared to control group.



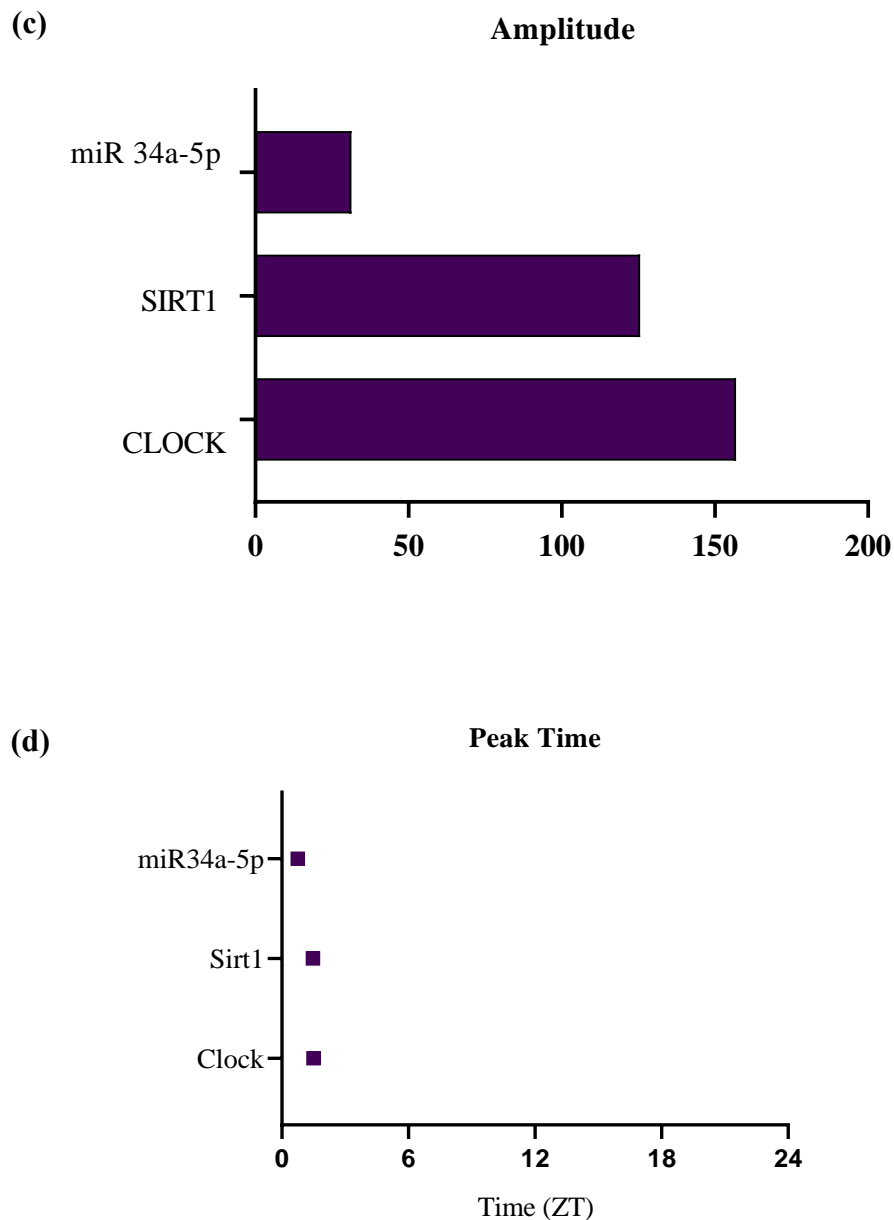


Fig. 2.3: Circadian rhythm of miR34a-5p and its target genes in thoracic aorta of C57BL/6J mice Thoracic aortae of mice were collected at different time points (ZT 0, 6, 12, 18 & 24). Expression of miR34a-5p and its target genes Clock and Sirt1 (a) mRNAs and (b) proteins were assessed for circadian pattern. CircWave software was used to analyse the (c) amplitudes and (d) peaks of this miRNA-mRNA couples (n=5).

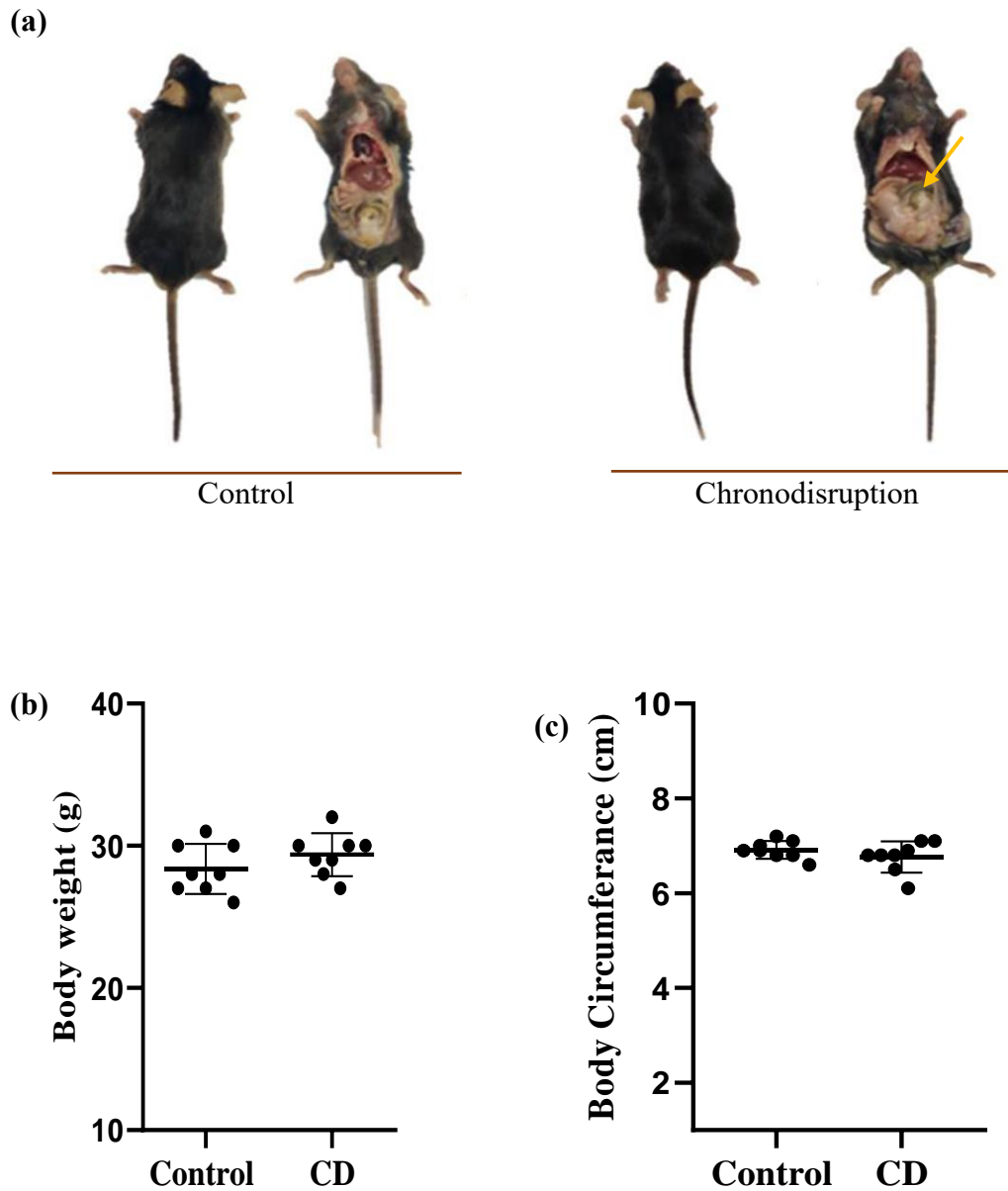


Fig. 2.4: Physiological traits of C57BL/6J mice (a) Autopsy of mice, arrow indicating visceral adipose deposit in chronodisruptive mice. The graphs represent (b) body weight and (c) body circumference of mice at the end of experimental protocol (n=7).

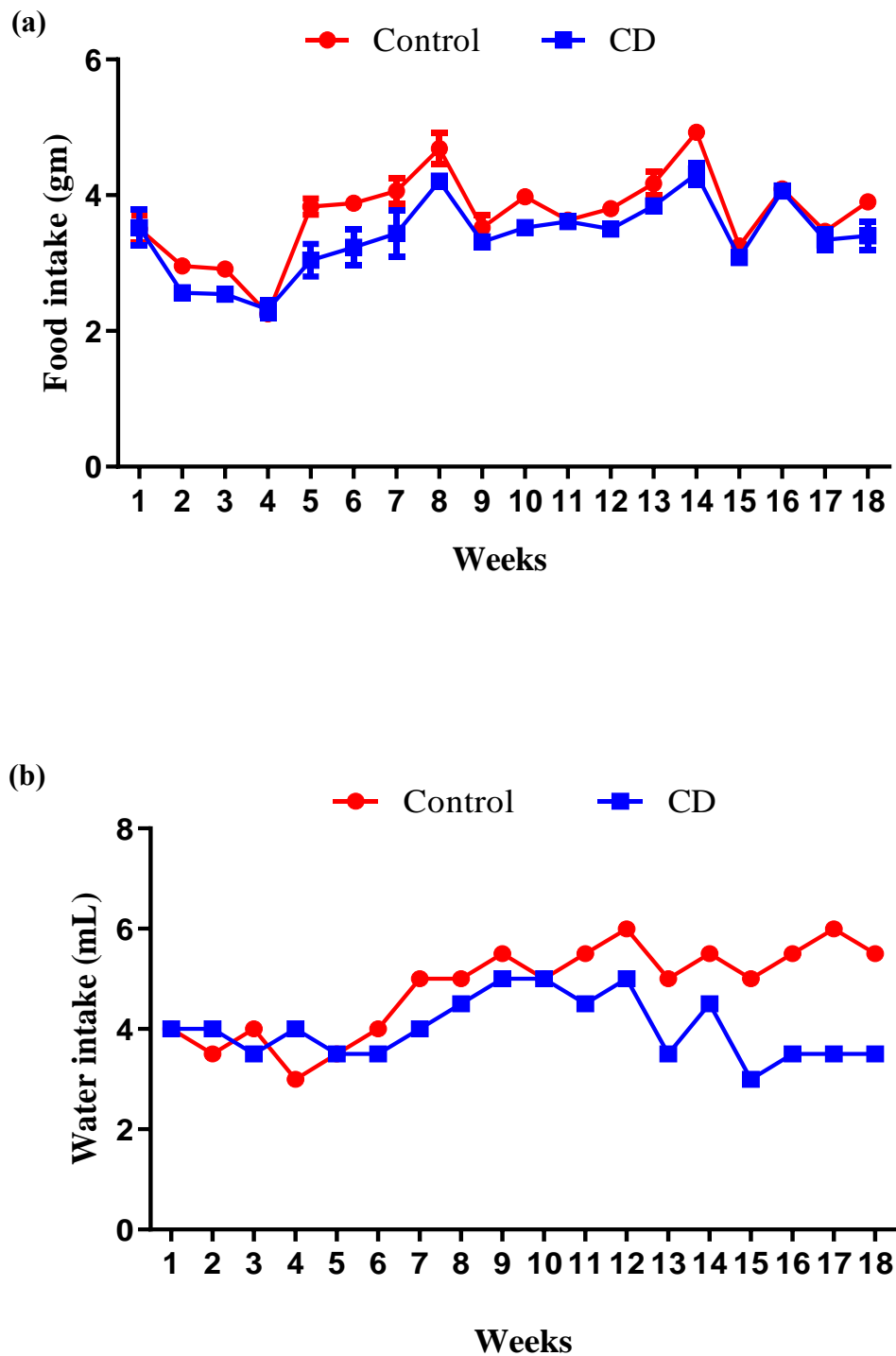


Fig. 2.5: Food and water intake of C57BL/6J mice. The graphs represent continuous measurement of (a) food intake and (b) water intake evaluated throughout the experiment.

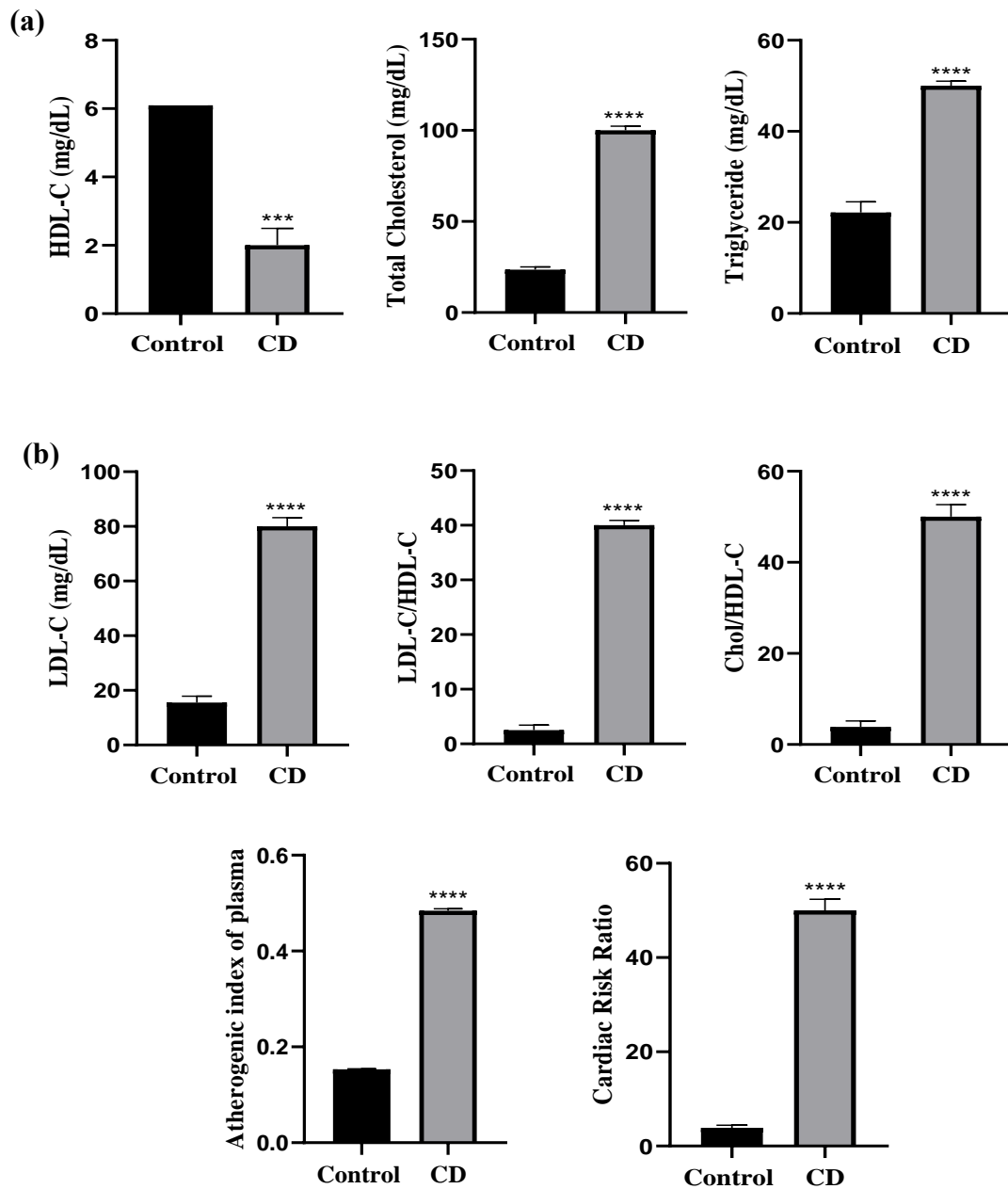


Fig. 2.6: Serum Lipid profile of C57BL/6J mice. (a) The graphs represent High Density Lipoprotein (HDL), Total Cholesterol (TC), Triglycerides (TGs), Low Density Lipoproteins (LDL) and ratios LDL/HDL and Chol/HDL respectively and (b) Atherogenic Index of plasma and Cardiac Risk Ratio (n=6). Results are expressed as mean \pm S.E.M. * p < 0.05, ** p < 0.01, *** p < 0.001 or **** p < 0.0001 is when CD is compared to control group.

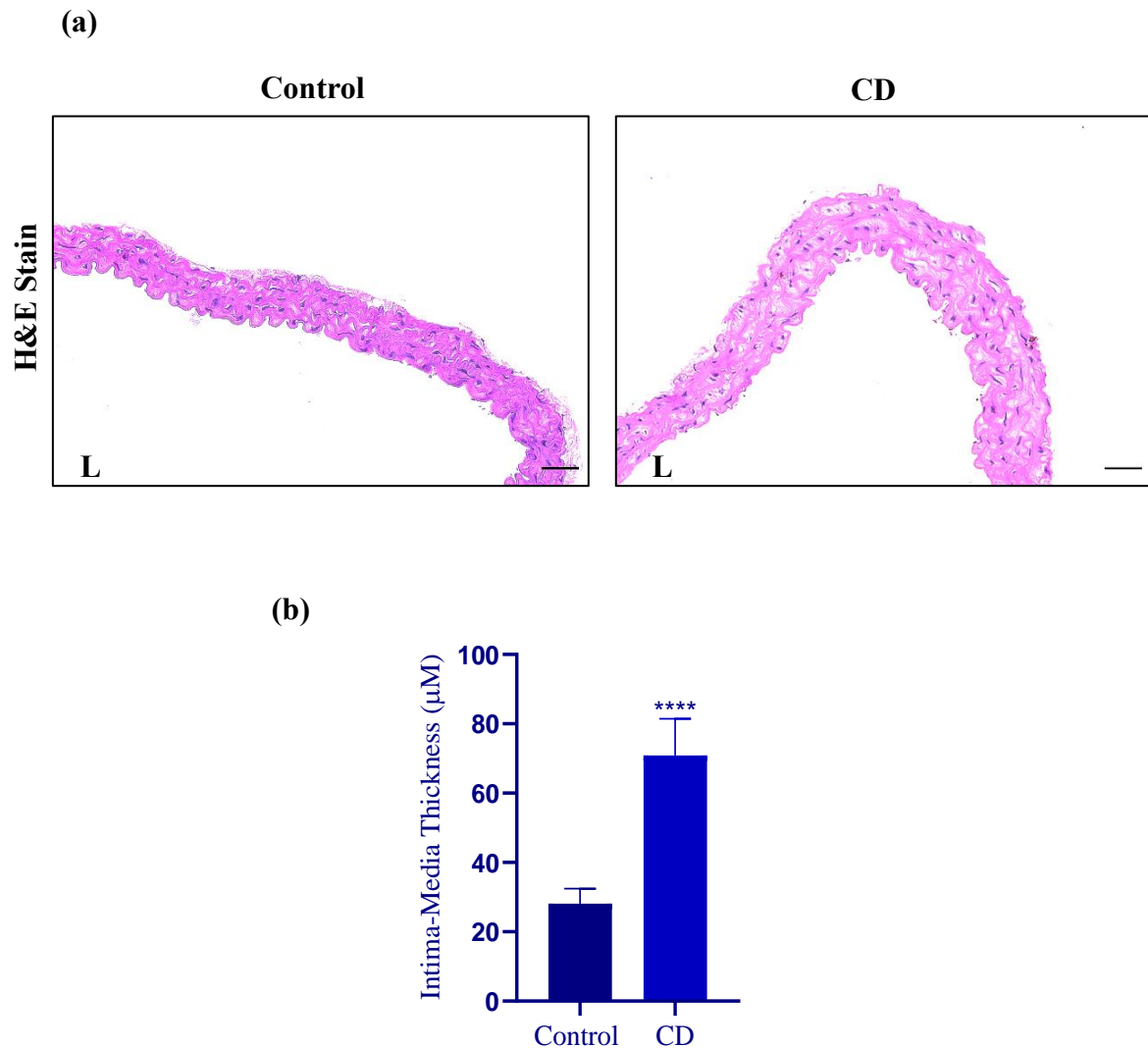


Fig. 2.7: Histomorphometric analysis of thoracic aortae of C57BL/6J mice. (a) Sections of thoracic aortae of mice were stained with Hematoxyline and Eosin stain (H&E); L represents luminal area. (Scale $100\mu\text{m}$; $n=3$) (b) Intima-Media thickness is represented graphically. Results are expressed as mean \pm S.E.M. $*p < 0.05$, $**p < 0.01$, $***p < 0.001$ or $****p < 0.0001$ is when CD is compared to control group.

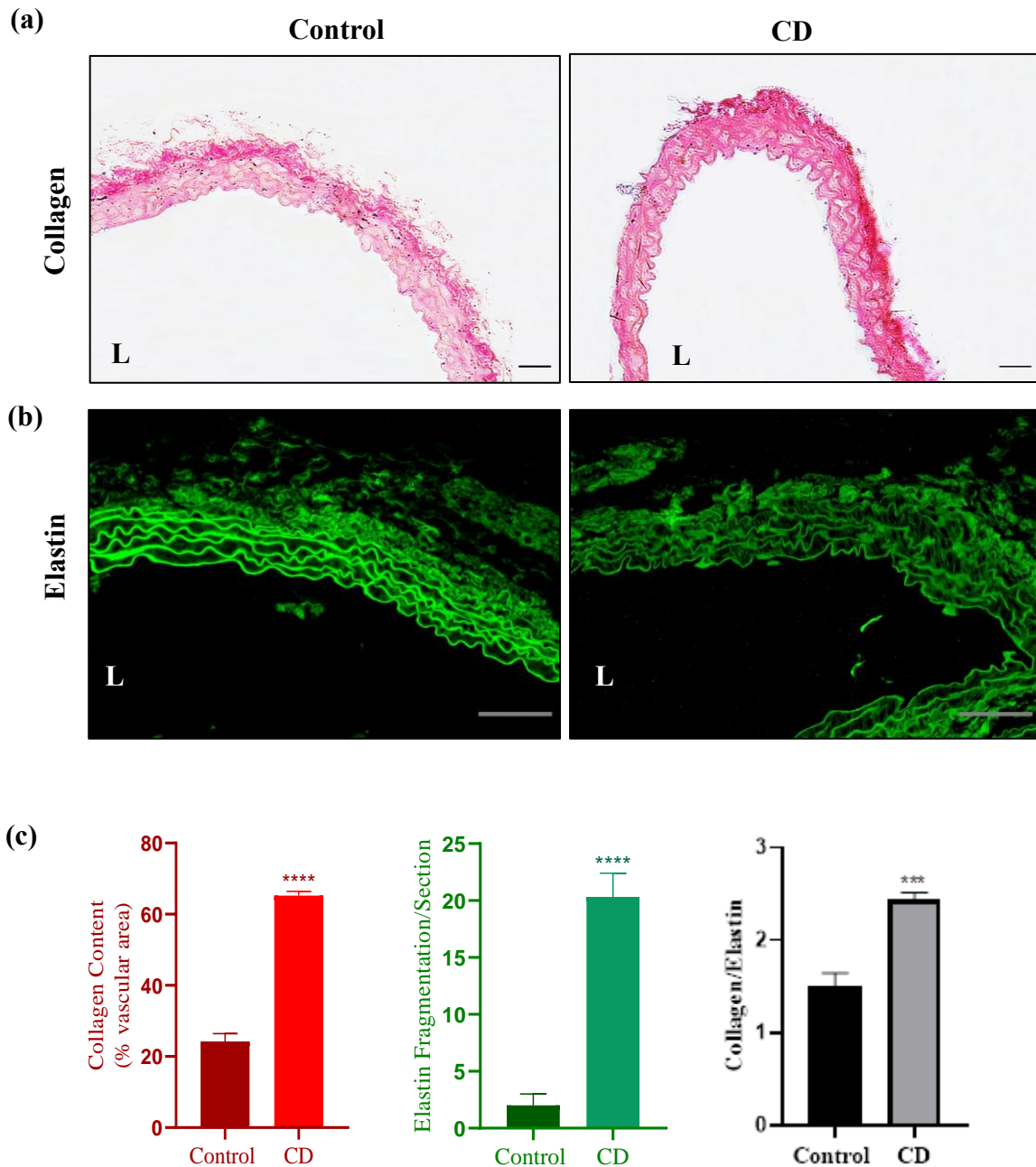


Fig. 2.8: Assessment of fibrillar content of the thoracic aortae. Thoracic aortae of C57BL/6J mice were (a) stained with Picrosirius Red stain to assess the collagen content in the vasculature and (b) elastin was evaluated with autofluorescence and fragmentations were observed per section. (c) The graphical representation of collagen content, elastin fragmentations per sections and collagen/elastin ratio are represented respectively (Scale 100 μ m; n=4). Results are expressed as mean \pm S.E.M. * $p < 0.05$, ** $p < 0.01$, *** $p < 0.001$ or **** $p < 0.0001$ is when CD is compared to control group.

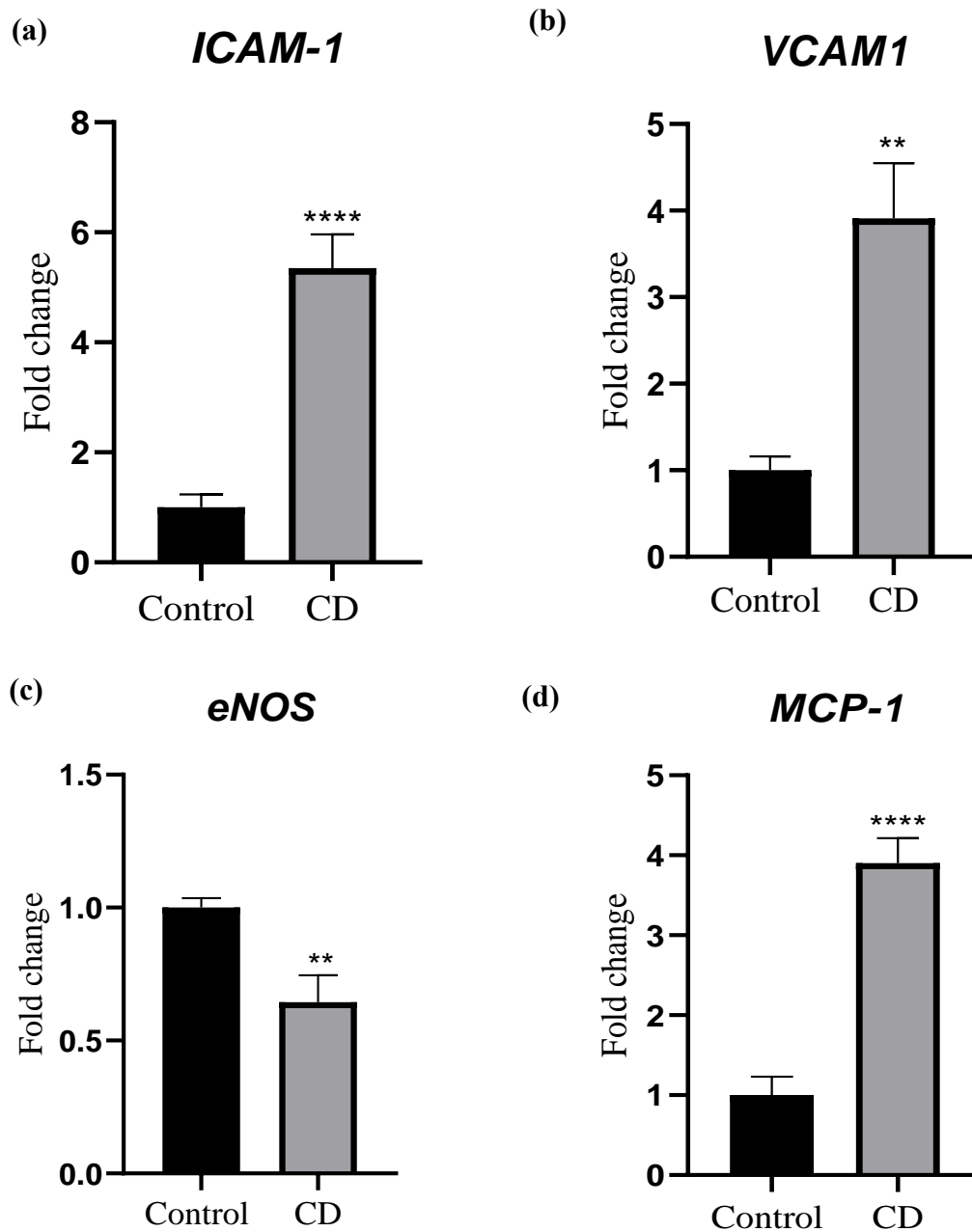
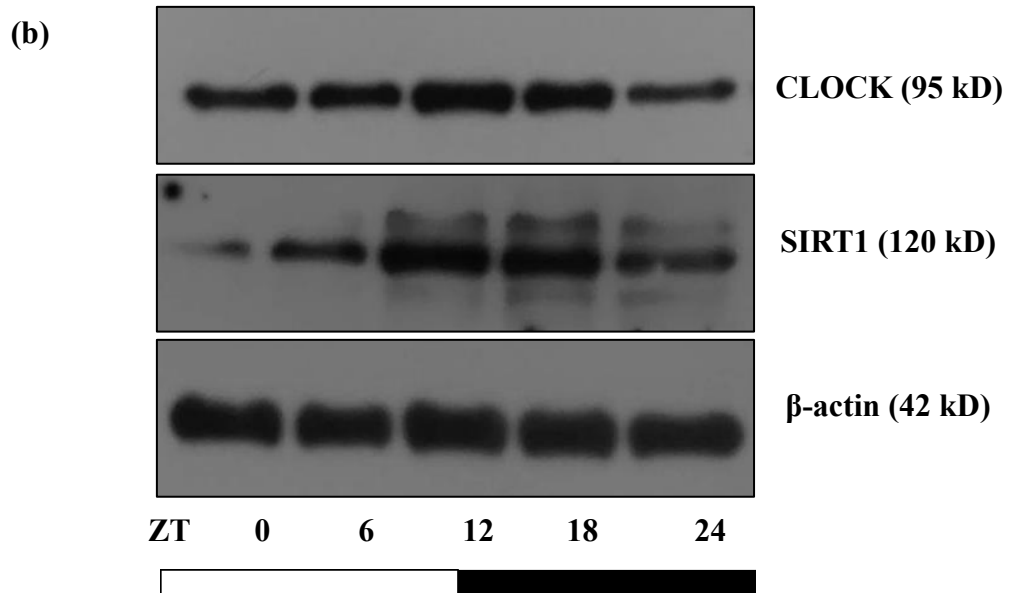
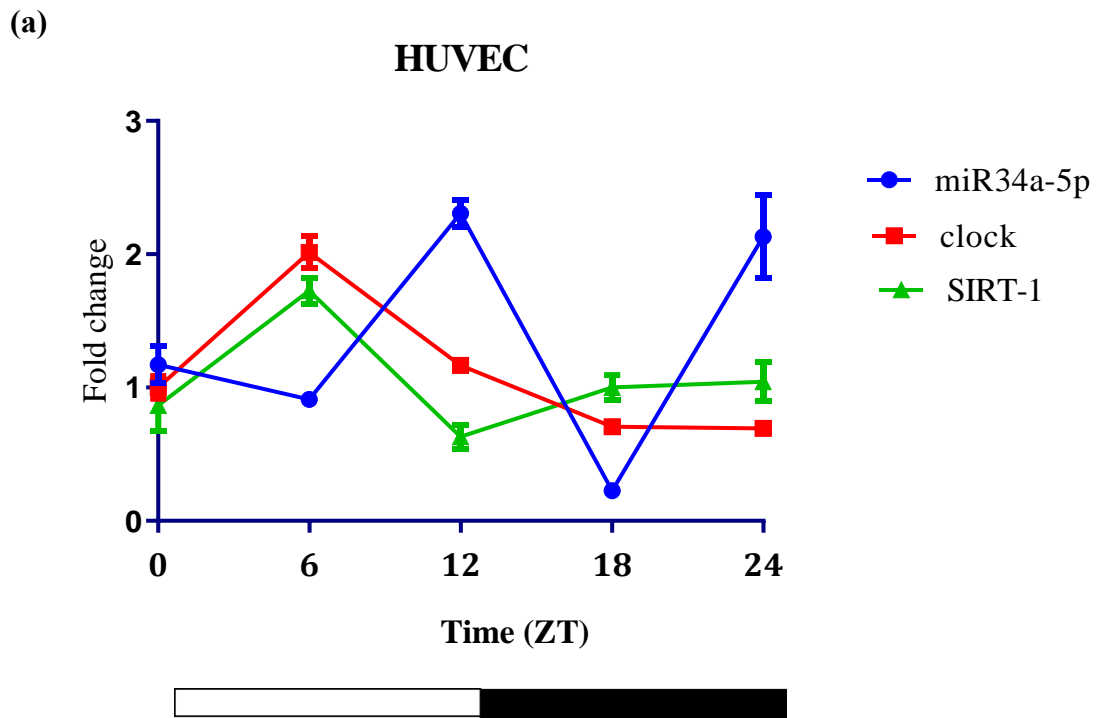


Fig. 2.9: Quantification of pro-atherogenic genes in thoracic aortae of C57BL/6J mice. Thoracic aortae of C57BL/6J mice were assessed for alterations in the mRNA levels of (a) ICAM-1 (b) VCAM-1 (c) eNOS and (d) MCP-1 using qPCR (n=6). Results are expressed as mean \pm S.E.M. * $p < 0.05$, ** $p < 0.01$, *** $p < 0.001$ or **** $p < 0.0001$ is when CD is compared to control group.



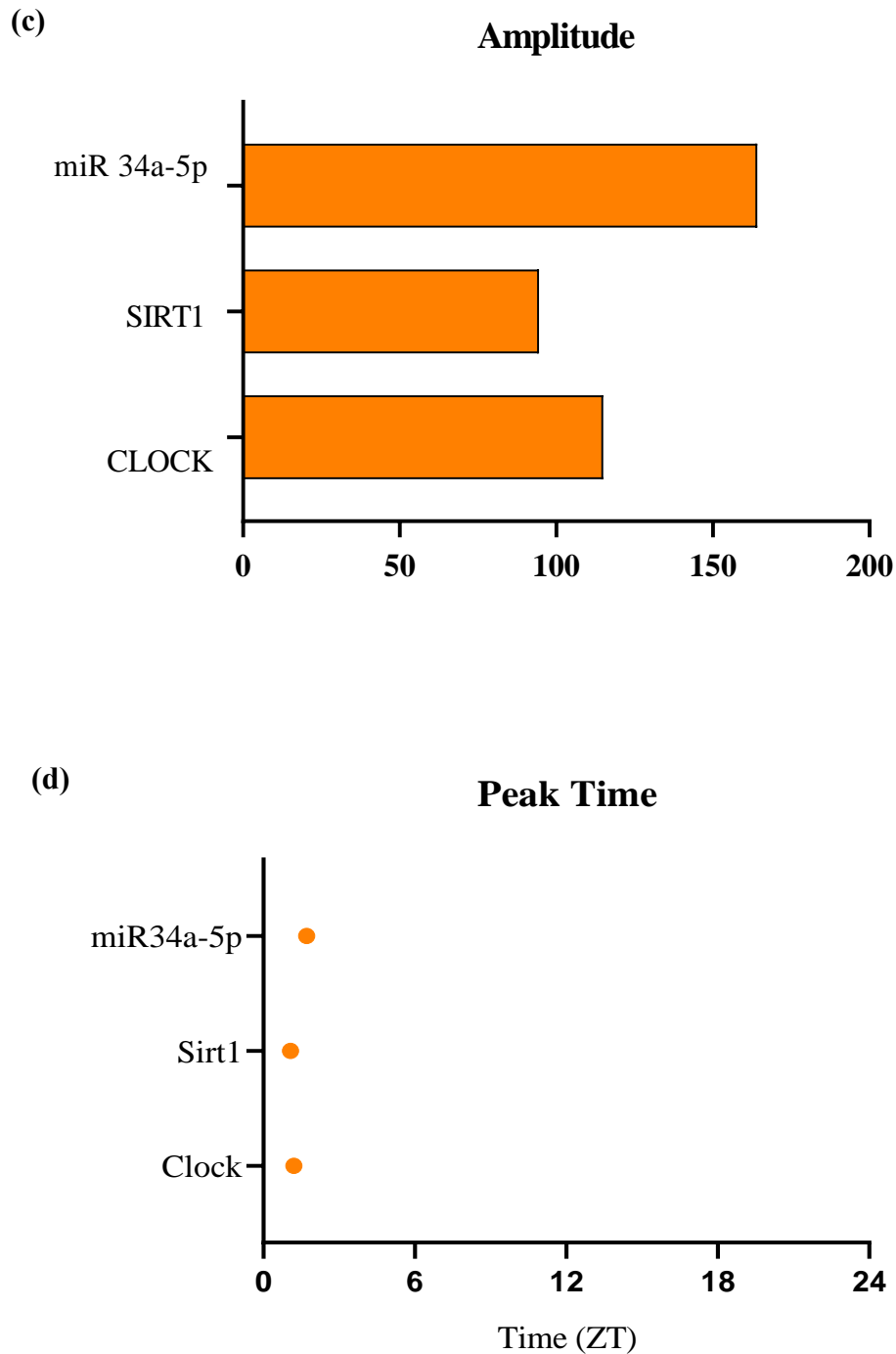


Fig. 2.10: Circadian rhythm of miR34a-5p and its target genes in HUVECs Synchronized HUVECS were harvested at different time points (ZT 0, 6, 12, 18 & 24). Expression of miR34a-5p and its target genes CLOCK and SIRT1 (a) mRNAs and (b) proteins were assessed for circadian pattern. CircWave software was used to analyse the (b) amplitudes and (c) peaks of this miRNA-mRNA couples (n=3).

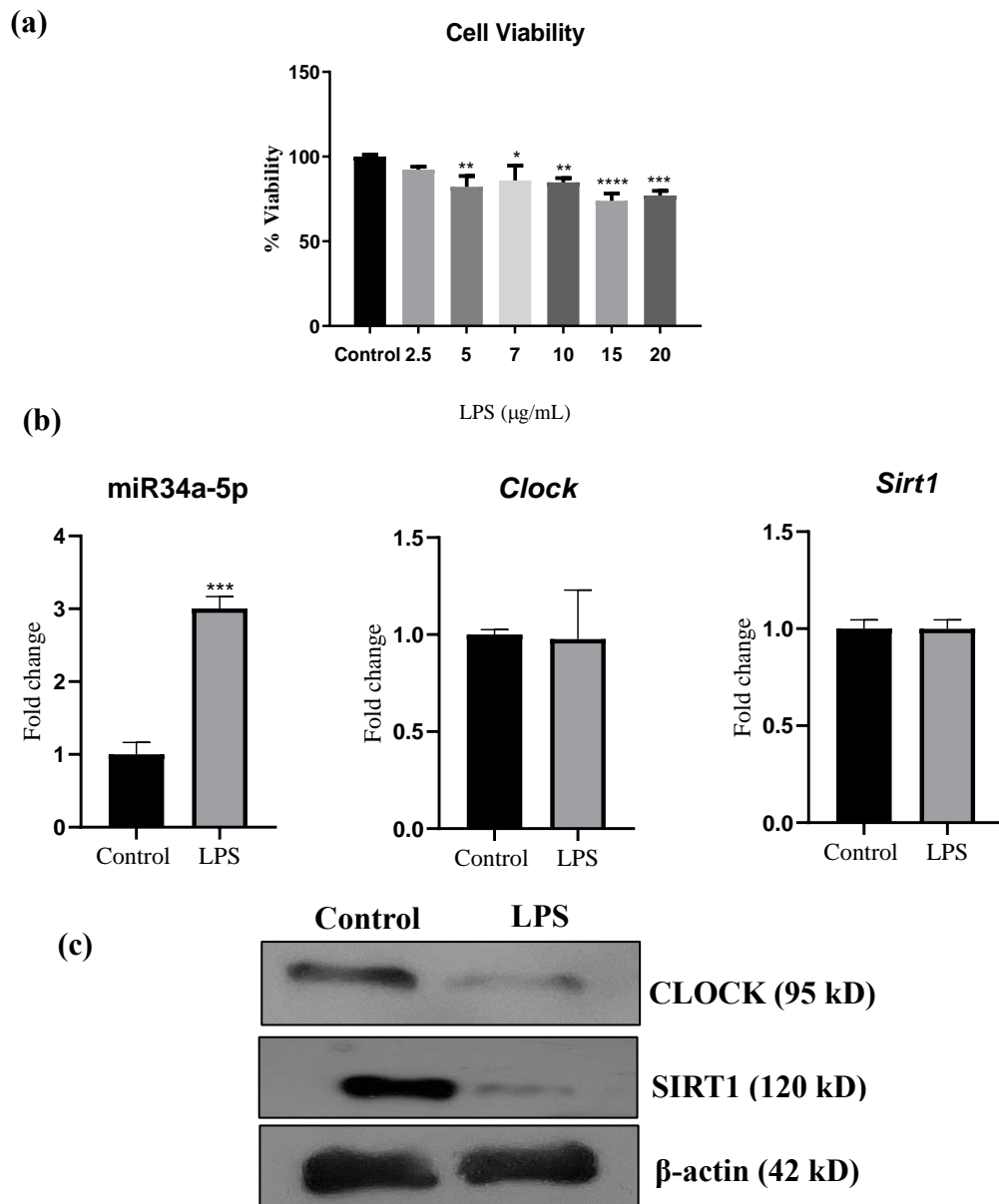


Fig. 2.11: Assessing Clock gene interaction in HUVECs with elevated miR34a-5p

(a) Different concentrations of LPS (2.5, 5, 7, 10, 15 & 20 µg/mL) were dosed to HUVECs for 24h to assess its cytotoxicity with MTT assay. (b) Levels of miR34a-5p and *CLOCK* and *SIRT1* transcripts were quantified with qPCR. (c) Immunoblot analysis *CLOCK* and *SIRT1* was done with β-actin as internal control (n=3). Results are expressed as mean ± S.E.M. * $p < 0.05$, ** $p < 0.01$, *** $p < 0.001$ or **** $p < 0.0001$ is when treated group is compared to the control group.

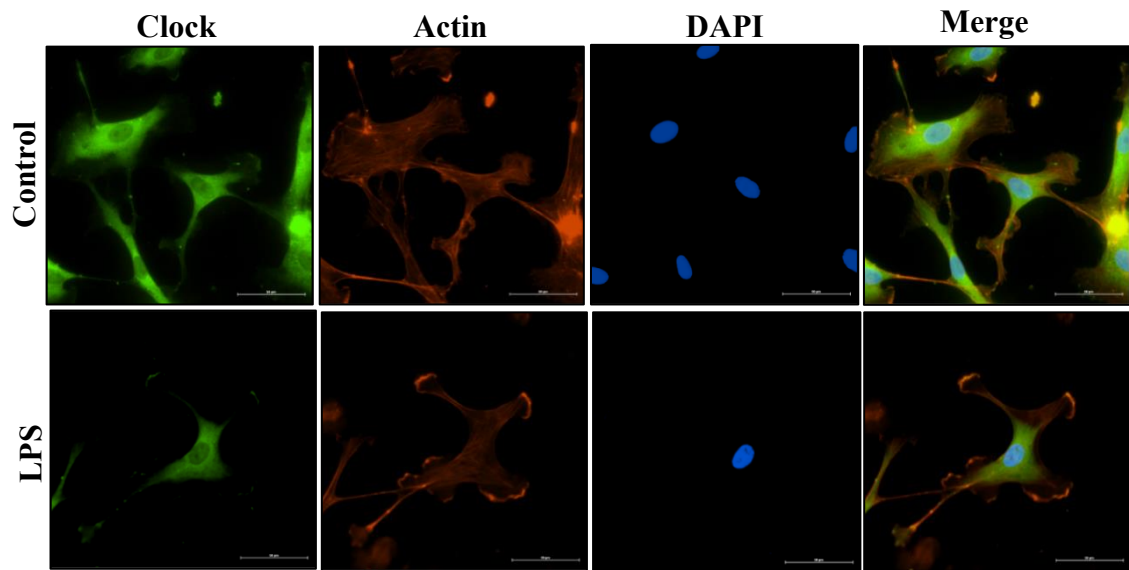


Fig. 2.12: Immunocytochemical analysis for CLOCK gene in LPS treated HUVECs Synchronized HUVECs were treated with LPS for 24h and processed for immunocytochemistry. The colors indicate following; Green: CLOCK, Red: β -actin, Blue: nucleus.

Discussion

In recent years, miRNAs have emerged as key regulators of fine-tuned gene expression in several physiological and pathological processes. miRNAs are cell-type enriched and operate by regulating gene network dynamically and/or transiently (i.e., by feed forward loop, feedback loop), along with steady state gene regulation (translational/transcriptional control). The regulatory control of miRNAs on circadian genes implies towards a possibility of those miRNAs exhibiting oscillations in synchrony with the circadian genes. In order to validate the computationally established circadian relation of miR34a-5p, a set of in-vivo experimentation was done with C57BL/6J mice. 6–8-week-old male mice were subjected to constant phase advance/phase delay photoperiodic manipulation for 18 weeks aiming to develop chronodisruption (Joshi, 2021). Assessment of systemic chronodisruption was done by evaluating circadian clock gene transcripts and protein content in the thoracic aorta of C57BL/6J mice. The same was further validated by immunohistochemical analysis of CLOCK gene in the thoracic aorta. Further analyzing miR34a-5p titers revealed elevation in the thoracic aorta of CD mice as compared to control. Chronodisruption induced aberrant methylation is well documented in the biological systems (Bollati *et al.*, 2010; Salazar *et al.*, 2018; Haim *et al.*, 2019). In order to elucidate the elevated miR34a-5p levels we evaluated the methylation pattern in its promoter region, at about 300 bp upstream of the transcription start site. Wherein we found alteration in the form of hypomethylation in the thoracic aorta of CD mice as compared to that of control, explaining the higher transcription rate and thus elevated levels of miR34a-5p.

Aortic vasculature comprises of tunica intima, tunica media and tunica adventitia. Intimal layer is in direct contact with the environment and primary site of lesion

formation (Stary *et al.*, 1994). To further investigate the circadian association to atherogenic pathology we aimed at investigating intima comprising of endothelial cells. Serum synchronized HUVECs were used for further invitro experimentations. In order to modulate gene expression in rhythmic fashion, miRNAs themselves might exhibit circadian expression. Gao *et al.*, 2016 showed miR17-5p, inhibiting Clock gene expression, exhibit circadian pattern in synchrony with clock gene (Gao *et al.*, 2016). Zhou *et al.*, 2020 showed miR 183/96/182 cluster to modulate the circadian rhythms by directly targeting period gene *PER2* (Zhou *et al.*, 2021). Herein, we aimed to assess circadian pattern, if any, of miR34a-5p in correspondence to its target Clock and Sirt1. To ascertain the same, thoracic aorta of C57BL6/J mice were collected in a time dependent manner at ZT 0, 6, 12, 18 & 24. A circadian pattern was observed in Clock and Sirt1, however the expression of miR34a-5p lacked any such rhythmic expression. Circadian rhythmic expression of miR34a has been reported in cancerous cell lines (Han *et al.*, 2016). Also, modulation of certain miRNAs is known to alter the phase and amplitude of circadian clock genes (Cheng *et al.*, 2007). These two sets of studies underline the fact that miRNAs too have a circadian cycle in synchrony with the core and peripheral clock genes. Oscillations of miR182/96/183 have been reported in U2OS cells, SCN, lung and retinal tissue. An inverse correlation and oscillatory pattern of miR-34a and *Per1* has also been shown in Mz-ChA-1 cells. miR17-5p has also been reported for its reciprocal regulation of CLOCK gene by binding at two sites on its 3'UTR in N2a cells and suprachiasmatic nucleus of mice. Our study is the first to report the cyclic expression of miR34a-5p in synchronized HUVEC cells. We report a reciprocal oscillatory relationship between *CLOCK / SIRT1* and miR34a-5p. The peak timings of *CLOCK / SIRT1* corresponded to the ebb of miR 34a-5p and vice-versa. Contrary to this observation, a similar oscillatory pattern of miR34a-5p was not seen in

thoracic aorta. Herein, amplitude of miR34a-5p was significantly higher in healthy HUVEC than in the aorta. However, amplitudes of *CLOCK* and *SIRT1* showed a synchronous pattern in both HUVEC as well as thoracic aorta. The peak timings quantified as COG values of *CLOCK*, *SIRT1* and miR34a-5p were similar and comparable. Dampened oscillations of miR34a-5p recorded in thoracic aorta is possibly attributable to its complex tissue architecture comprising of diverse cell types in which, the tunica intima contributes to a small subset of the total mass and fail to put out the sole cellular settings.

miR34a-5p – *CLOCK* association was further assessed with LPS induced upregulation of miR34a-5p. This had accounted for complete loss of cyclicity of *CLOCK* and *SIRT1* expressions, plausibly pertaining to constantly elevated cellular levels of miR34a-5p impeding the translational process. *SIRT1*, a known target of miR34a-5p, deacetylates *BMAL1* and facilitates *CLOCK*-*BMAL1* heterodimerization that further transcribes peripheral clock genes (*Per1*, *Per2*, *Cry1*, *Cry2*, *Cry3*) and deacetylates *Per2* that completes the feedback loop by inhibiting transcription of peripheral clock genes. Moreover, miR34a-5p is also documented to bind to 3'UTR and not only inhibit *PER2* expression but consequentially shorten the period of circadian length. The luciferase reporter gene analysis confirmed miR34a-5p mediated inhibition of *CLOCK* gene expression. The observed higher levels of miR34a-5p had accounted for imperative perturbations in circadian clock expression in HUVEC and therefore miR34a-5p can be proposed as a potential chronodisruptive miRNA.

Chronodisruption is claimed to be one of the major causing factors of cardiovascular disorders. Several studies have shown circadian bases of cardiovascular disorders in light of blood pressure regulation, cases of heart attacks, pacing heart rates etc. Herein, we looked for pro-atherogenic manifestations in the thoracic aorta of chronodisruptive

C57BL/6J mice. Primary evaluation of serum lipid profile unveiled higher AIP and CRR in CD mice as compared to the control, marking initial peril of onset of CVDs. Further details were procured from histo-morphometric analysis that showed higher intima-media thickness in the thoracic aortae of CD mice. Intima-media thickening is a prominent pro-atherogenic feature that is studied as one of the markers of arterial remodelling (O'Leary and Polak, 2002). In addition to that, extensive elastin fragmentation along with increased collagen deposition in the media and adventitia accounted for a higher collagen-to-elastin ratio. These changes often compromise the vascular function and distensibility increasing the arterial rigidity (Li *et al.*, 2018a). These pro-atherogenic traits were further confirmed at molecular level by gene expression studies. The structural changes in arterial wall and the related functional alterations are known to be resulting from underlying endothelial dysfunction. Monolayer of ECs forms the intima of the vascular wall and places them in direct contact of the environment. ECs are more susceptible and responsive to damage by external stressors. ECs produce NO for regulating vasomotor tone by eNOS enzyme that showed compromised production in thoracic aortae of CD mice. In stressed conditions activated EC present adhesion molecules (ICAM-1 and VCAM-1) on their cell membrane and produce protein MCP-1 responsible for recruiting monocytes to subintimal space and marking the initiation of atherosclerosis (Piga *et al.*, 2007). Thoracic aorta of CD mice displayed higher levels of ICAM-1, VCAM-1 and MCP-1 as compared to the control.

Physiologically SIRT1 is positioned at a chrono-metabolic juncture and is reported to be functional at several stages of initiation and development of atherosclerosis (Soni *et al.*, 2021). Loss of SIRT1 impacts endothelial migration, apoptosis, inflammation, vasodilation, lipid flux and arterial remodeling in atherogenic pathology. Elevated

levels of miR34a-5p have been reported as a major cause for lowered SIRT1 expression as it binds to its 3'UTR (Tabuchi *et al.*, 2012; Castro *et al.*, 2013; Kim *et al.*, 2015). Over all, this study confirms the miR34a-5p based regulation of CLOCK gene expression in synchronized endothelial cells along with the inhibition of SIRT1 expression which makes it a potential link in chronodisruption induced atherosclerosis.